Oligonucleotides forming an i-motif: the pH-dependent assembly of individual strands and branched structures containing 2′-deoxy-5-propynylcytidine†‡

Frank Seela,*[a,b] Simone Budow[a,b] and Peter Leonard[a,b]

Received 27th March 2007, Accepted 17th April 2007
First published as an Advance Article on the web 10th May 2007
DOI: 10.1039/b704583b

Non-branched and branched oligonucleotides incorporating consecutive runs of 2′-deoxy-5-propynylcytidine residues (**2**) instead of 2′-deoxycytidine (**1**) were synthesized. For this, phosphoramidite building blocks of 2′-deoxy-5-propynylcytidine (**3a–c**) were prepared using acetyl, benzoyl or *N*,*N*-di-*n*-butylaminomethylidene protecting groups. The formation of the i-motif assemblies incorporating 2′-deoxy-5-propynylcytidine residues was confirmed by temperature-dependent CD- and UV-spectra as well as by ion-exchange chromatography. The low pK_a-value of nucleoside **2** (pK_a = 3.3) compared to dC (pK_a = 4.5) required strong acidic conditions for i-motif formation. Branched oligonucleotide residues with strands in a parallel orientation lead to a strong stabilization of the i-motif allowing aggregation even at non-optimal pH conditions (pH = 5). The immobilization of oligonucleotides incorporating multiple residues of **2** on 15 nm gold nanoparticles generated DNA–gold nanoparticle conjugates which are able to aggregate into i-motif structures at pH 5.

Introduction

Cytosine-rich regions are frequently found in the human genome located near or within regions of functional or regulatory importance including the centromer and telomer domains as well as the insulin minisatellite.[1–8] They are assumed to play an important biological role in genetic regulation processes.[4,6,9] The formation of parallel duplexes stabilized by hemiprotonated cytosine–cytosine base pairs was reported for the crystals of polycytidylic acid even forty years ago.[10] Later, NMR studies and X-ray analyses of cytosine-rich oligonucleotides showed that the formation of a four-stranded molecule is stabilized by the intercalation of non-canonical hemiprotonated cytosine–cytosine base pairs (dCH$^+$·dC) of two parallel-stranded duplexes (Fig. 1).[6,11–14] Due to the intrinsic cytosine intercalation this structure was named an "i-motif". Consistent with the hemiprotonation of the cytosine residues, the i-motif assembly occurs under weakly acidic or even under nearly neutral conditions.[6] i-Motif structures are formed by association of four separate strands, by two hairpins or branched oligonucleotides containing two cytosine-rich stretches, or by intramolecular folding of a single strand employing four dC stretches.[4,11–16]

Branched oligonucleotides are important components of RNA molecules. It is well known that branching points act as structural key points in pre-mRNA splicing and as protein binding sites.[17–18] The construction of "V"-shaped branched cytosine-rich DNA-oligonucleotides employing a riboadenosine linker was reported earlier.[19–20] Several backbone modifications have been performed to probe the structural features of the i-motif including those of (i) phosphorothioates,[21–22] (ii) 3′-*S*-phosphorothiolates,[23] (iii) methylphosphonates[22,24] and (iv) 3′-*N*-phosphoramidates.[24] However, only in the case of the 3′-*S*-phosphorothiolate was a considerable stabilization of the i-motif structure observed.[23] Very little is known about cytosine nucleobase analogues forming an

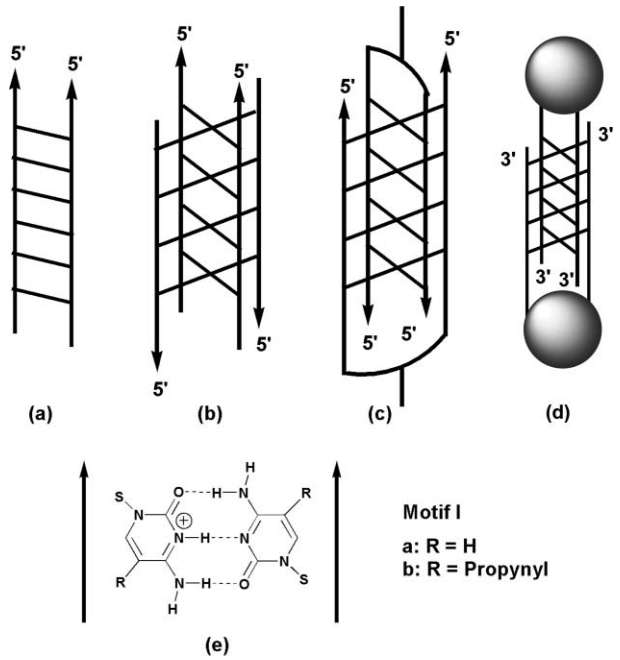

Fig. 1 Schematic representation of a hemiprotonated duplex (a), a tetrameric i-motif (b), a two-fold branched i-motif (c) and an i-motif structure conjugated to gold nanoparticles (d). The assemblies are stabilized by hemiprotonated cytosine base pairs (e). S corresponds to the 2′-deoxyribofuranosyl sugar moiety.

[a]*Laboratory of Bioorganic Chemistry and Chemical Biology, Center for Nanotechnology, Heisenbergstraße 11, 48149, Münster, Germany*
[b]*Laboratorium für Organische und Bioorganische Chemie, Institut für Chemie, Universität Osnabrück, Barbarastraße, 7, 49069, Osnabrück, Germany. E-mail: Frank.Seela@uni-osnabrueck.de, Seela@uni-muenster.de; Web: www.seela.net; Fax: +49 (0)251 53406 501; Tel: +49 (0)251 53406 500*

† The HTML version of this article has been enhanced with colour images.
‡ Electronic supplementary information (ESI) available: HPLC profiles. See DOI: 10.1039/b704583b

i-motif.[15,24–25] However, the crystallographic data of the i-motif structure indicates that the position-5 of the cytosine residues has steric freedom and therefore modifications at that position should be tolerated.

As a part of our studies on multi-stranded DNA structures, we became interested in introducing cytosine analogues carrying a side chain modification such as the propynyl group into the i-motif structure. However, it was unclear whether the i-motif is able to accept such a bulky residue. This manuscript reports on i-motif structures of oligonucleotides incorporating consecutive runs of 2′-deoxy-5-propynylcytidine (**2**) instead of 2′-deoxycytidine (**1**). For this purpose, the phosphoramidites of 2′-deoxy-5-propynylcytidine (**3a–c**) were synthesized (Fig. 2). Particular attention was focused on i-motif structures formed by four individual strands as well as on i-motifs formed by branched oligonucleotides or immobilized on gold nanoparticles (Fig. 1a–d). The formation of the modified i-motif structures (Fig. 1e) was directly proved by spectroscopic techniques, ion-exchange chromatography and the reversible aggregation of the nanoparticle–DNA conjugates.

Results and discussion

1. Synthesis of the monomers

The 2′-deoxy-5-propynylcytidine (**2**) is well known to stabilize duplex and triplex nucleic acids.[26–29] Thus, numerous reports on the application of 2′-deoxy-5-propynylcytidine as a T_m-enhancer have been published.[26–29] However, to the best of our knowledge no detailed information on the synthesis of the phosphoramidite of 2′-deoxy-5-propynylcytidine (**2**) is available in the literature.[30] As we encountered certain problems during synthesis, we now report on the full details of the synthesis of the phosphoramidite building blocks **3a–c**. 2′-Deoxy-5-iodocytidine (**4**) was converted to the propynylated nucleoside **2** under standard conditions *via* the palladium(0)-catalyzed Sonogashira cross-coupling reaction in the presence of copper iodide and propyne gas (88% yield, Scheme 1). The propynylated nucleoside **2** shows a strong downfield shift for carbon C5 compared to the starting material **4**, while only minor changes are observed for the other carbon signals (Table 1).

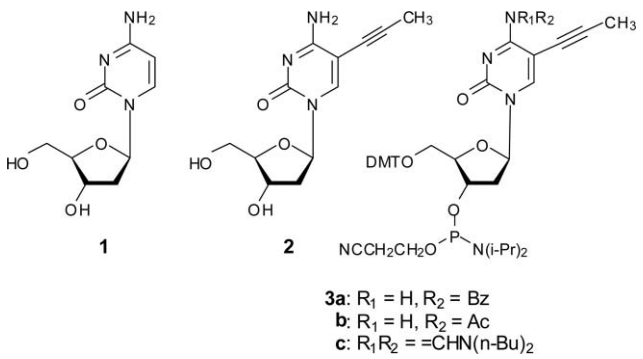

Fig. 2 Structures of nucleosides and the corresponding phosphoramidites.

For the amino group protection, the acetyl, benzoyl and *N*,*N*-di-*n*-butylaminomethylidene groups were chosen to fulfil the various requirements of oligonucleotide synthesis including (i) fast deprotection, (ii) standard oligonucleotide synthesis or (iii) introduction of lipophilic residues. Although the reaction could be monitored by TLC, very little material was obtained after flash chromatography. This was different from the 2′-deoxycytidine nucleoside, which afforded the acetylated derivative in sufficient yield.[31] The electron-withdrawing property of the propynyl side chain increases the amide character of the amino group. This is indicated by the lower pK_a-value of the modified nucleoside thereby the stability of the amino protecting groups is affected. Thus, the 5′-hydroxyl group of **2** was blocked first (4,4′-dimethoxytrityl chloride in pyridine) giving the DMT-derivative **5** in 80% yield. Afterwards the more lipophilic **5** was protected with the acetyl, benzoyl or *N*,*N*-di-*n*-butylaminomethylidene residues (69% for **6a**, 80% for **6b**, 67% for **6c**). The stability of the amino protecting groups increases in the order acetyl < benzoyl < *N*,*N*-di-*n*-butylaminomethylidene in aqueous ammonia or methanol at room temperature as indicated by TLC monitoring. Phosphitylation of the intermediates **6a–c** with (2-cyanoethyl)diisopropylphosphoramido chloridite afforded the phosphoramidites **3a–c** (63–68% yield). All compounds were characterized by their UV spectra, ^{13}C- and ^{1}H-NMR spectra, as well as by elemental analysis (see Table 1 and the Experimental section).

2. Properties of the monomers

The single-crystal X-ray analysis of 5-propynyl-2′-deoxycytidine (**2**) revealed that in the solid state the propynyl side chain is linear and rigid.[33] We noticed that the introduction of the propynyl group at position-5 of the pyrimidine moiety lowers the pK_a value from 4.5 (2′-deoxycytidine) to 3.3 (nucleoside **2**). This phenomenon has already been discussed for triplex-forming oligonucleotides incorporating 5-propynyl-2′-deoxycytidine residues.[26] For this, UV-spectra of the nucleosides **1** and **2** were measured in a 0.3 M NaCl, 10 mM phosphate buffer solution at pH 3.5 and pH 7 (Fig. 3). The canonical nucleoside 2′-deoxycytidine shows a characteristic UV maximum at 279 nm at pH 3.5, whereas under neutral conditions

Table 1 ^{13}C-NMR chemical shifts (in ppm) of the nucleosides and their derivatives measured in d_6-DMSO at 298 K[a]

	C(2)	C(4)	C(5)	C(6)	C≡C	CH_3	C=O/N=CH	C(1′)	C(2′)	C(3′)	C(4′)	C(5′)	DMT	OMe
1[b]	155.2	165.5	94.1	141.1	—	—	—	85.0	40.4	70.5	87.2	61.5	—	—
2	153.4	164.3	90.7	143.4	71.1, 91.8	4.4	—	85.2	40.4	70.1	87.4	61.0	—	—
4	153.8	163.6	56.5	147.2	—	—	—	85.2	40.7	69.8	87.3	60.8	—	—
5	153.3	164.3	90.8	144.7	70.7, 91.5	4.2	—	85.2[c]	40.7	70.5	85.8[c]	63.6	85.6	55.0
6a	n.d.	n.d.	90.8	144.7	71.2, n.d.	3.9	167.2	85.8[c]	40.4	70.1	86.1[c]	63.4	n.d.	55.0
6b	152.3	160.7	93.3	144.7	69.7, 93.3	25.3, 4.2	170.2	85.9[c]	40.4	70.1	86.7[c]	63.3	86.2	55.0
6c	153.4	170.1	87.9	144.8	73.3, 98.8	3.9, 13.5	157.3	85.7[c]	40.9	70.5	85.8[c]	63.6	n.d.	55.0

[a] Systematic numbering is used, n.d. = not detected. [b] From ref. 32. [c] Tentative.

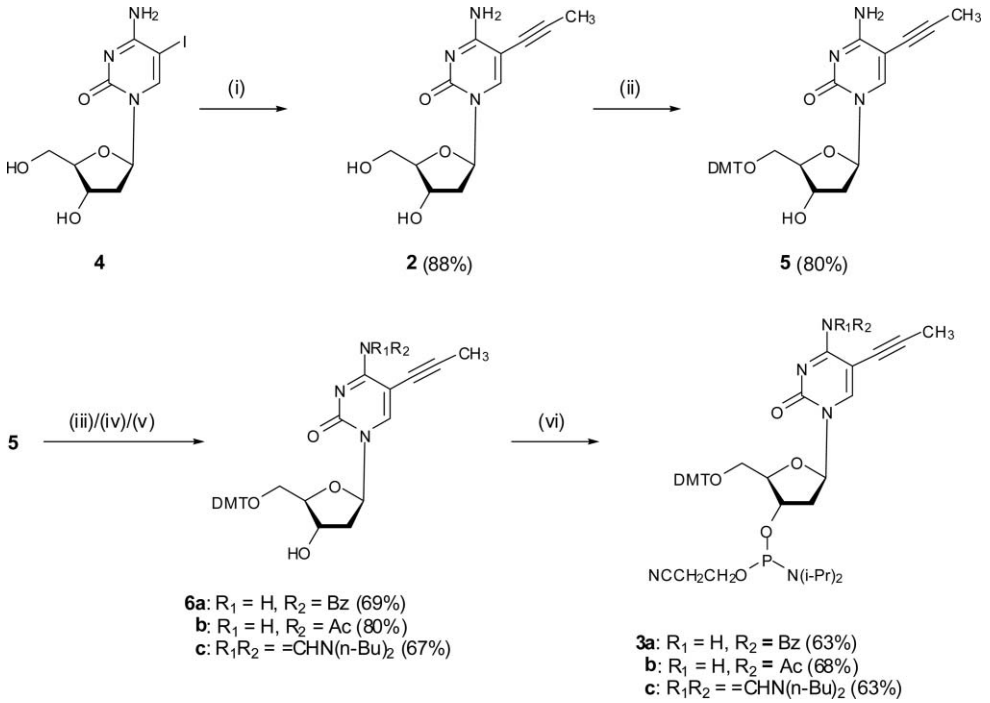

Scheme 1 *Reagents and conditions*: (i) propyne, Pd(0) catalyst, CuI; (ii) DMTr-Cl, pyridine, overnight, r.t.; (iii) Bz_2O, pyridine, overnight, r.t.; (iv) Ac_2O, DMF, overnight, r.t.; (v) *N*,*N*-di-*n*-butylformamide dimethylacetal, methanol, 3 h, r.t.; (vi) (2-cyanoethyl)diisopropylphosphoramido chloridite, *N*,*N*-diisopropylethylamine, anhyd. CH_2Cl_2, 20 min, r.t.

(pH 7) the maximum is hypsochromically shifted to 271 nm. In contrast, the UV maxima of the 5-propynylated nucleoside **2** are bathochromically shifted at both pH values compared to the non-functionalized 2′-deoxycytidine, as indicated by Fig. 3. At pH 3.5, the UV maximum of nucleoside **2** is centred at 308 nm (Fig. 3a) and at pH 7 it is located at 290 nm (Fig. 3b).

3. Synthesis and characterization of the oligonucleotides

Next, a series of oligonucleotides was prepared as shown in Tables 2–4. The oligonucleotides **10–19** and **21** were synthesized by solid-phase synthesis employing the regular phosphoramidites and the phosphoramidite **3b**.[34] Some oligonucleotides were functionalized with a thiol linker group at their 3′- or 5′-termini which makes them suitable for the immobilization on the surface of gold nanoparticles.[35] For the 3′-thiol modification of **12**, **16** and **18** a 3′-thiol-modifier-C3 S–S CPG was used (Glen Research, US) whereas a 5′-thiol-modifier-C6-phosphoramidite (Glen Research, US) was employed for the 5′-thiol modification of **19** and **21**. The syntheses of the 3′-thiol and 5′-thiol modified oligonucleotides were carried out according to the standard procedure for solid-phase synthesis of oligonucleotides. The purification of the 3′-thiol modified oligonucleotides was performed by reversed-phase HPLC (RP-18) in the DMT-on modus, followed by deprotection with 80% acetic acid and precipitation with 1 M NaCl and ethanol in an ice-bath (for details see the experimental section). The 5′-thiol functionalized oligonucleotides **19** and **21** were only purified in the trityl-on modus (RP-18).

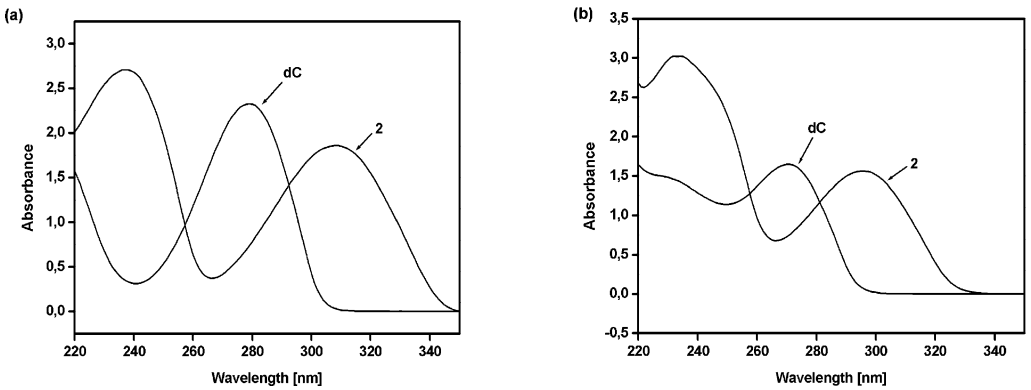

Fig. 3 UV spectra of nucleosides dC and **2** measured in a 0.3 M NaCl, 10 mM phosphate buffer solution at pH 3.5 (a) and pH 7 (b) at a concentration of 1.4×10^{-4} mol l^{-1}.

Table 2 The molecular masses of selected non-branched oligonucleotides determined by MALDI-TOF mass spectrometry

Non-branched oligonucleotides	$[M + H]^+$ (Da)	
	Calc.	Found
5′-d(T-T-**2**-**2**-**2**-**2**-T-T) (**11**)	2465	2466
5′-d[(T-T-**2**-**2**-**2**-**2**-**2**-**2**-T-T)-$(CH_2)_3$-S-S-$(CH_2)_3$-OH] (**12**)	3363	3363
5′-d{[Trityl-S-$(CH_2)_6$-O(PO_2H)O]-T-T-**2**-**2**-**2**-**2**-**2**-**2**-T-T} (**19**)	3558	3558
5′-d{[Trityl-S-$(CH_2)_6$-O(PO_2H)O]-(A-G-T-A-T-T-G-A-C-C-T-A)$_2$} (**21**)	7790	7790

For the syntheses of the branched oligonucleotides **13–18** the synthesis protocol was modified. The introduction of the branching residue (Glen Research, US) led to the formation of two parallel-stranded oligonucleotide chains. The elongation of the two growing oligonucleotide chains is performed in a parallel way, leading to identical sequences of both strands. Double-concentrated solutions (0.2 M instead of 0.1 M) of the phosphoramidite building blocks were employed during solid-phase synthesis, and the coupling time for each residue was extended. The purification was performed as described for the 3′-thiol-modified oligonucleotides. All oligonucleotides were characterized by MALDI-TOF mass spectra. The calculated masses were in good agreement with the measured values (Table 2 and Table 4). The composition of selected oligonucleotides was determined by HPLC (RP-18) after tandem enzymatic hydrolysis with snake-venom phosphodiesterase followed by alkaline phosphatase in 0.1 M Tris·HCl buffer (pH 8.9) at 37 °C. The HPLC profile of the hydrolysis products clearly demonstrates that the propynylated nucleoside **2** is much more hydrophobic compared to the non-functionalized dC (see Supporting information‡).

4. i-Motif formation of non-branched oligonucleotides

In the following discussion, non-branched oligonucleotides containing 2′-deoxycytidine or 2′-deoxy-5-propynylcytidine are compared. They were characterized by temperature-dependent circular dichroism (CD) spectra, ion-exchange chromatography and T_m measurements (for oligonucleotide sequences see Table 3). Cytosine-rich oligonucleotides forming i-motif structures such as 5′-d(T-T-C-C-C-C-T-T) (**8**) and 5′-d(T-T-C-C-C-C-C-C-T-T) (**9**) can be identified by their characteristic CD spectra. Both oligonucleotide assemblies produce positive Cotton effects around 280 nm which are accompanied by concomitant negative effects around 260 nm (for **8** see Fig. 4a). These spectral characteristics appear at pH 5 and disappear at elevated temperature due to the disassembly of the i-motif and are not formed under slightly

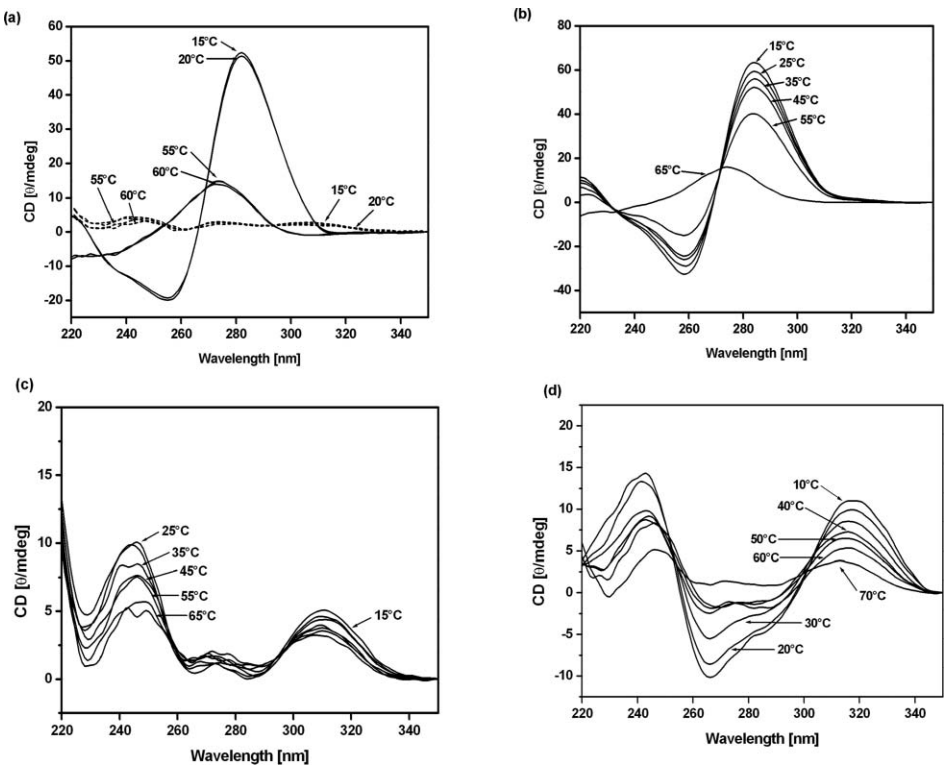

Fig. 4 CD spectra of the tetrameric i-motif structure formed by (a) 5′-d(T-T-C-C-C-C-T-T) (**8**; solid line) and 5′-d(T-T-**2**-**2**-**2**-**2**-T-T) (**11**; dashed line) at pH 5; (b) 5′-d(T-T-C-C-C-**2**-C-C-T-T) (**10**) at pH 5; (c) the single-stranded species of 5′-d[(T-T-**2**-**2**-**2**-**2**-**2**-**2**-T-T)-$(CH_2)_3$-S-S-$(CH_2)_3$-OH] (**12**) at pH 5 after 20 days incubation time; (d) the tetrameric i-motif assembly of **12** at pH 3.5 after 18 h incubation time. For the CD measurements, the oligonucleotides were dissolved in 0.3 M NaCl, 10 mM sodium phosphate buffer.

alkaline conditions (pH 8).[3,25] The i-motif formation was next probed on oligonucleotides containing 2′-deoxy-5-propynylcytidine (**2**). The replacement of one dC residue in oligonucleotide **9** by compound **2** led to the oligonucleotide **10**. The CD spectra obtained from oligomer **10** measured under the same conditions resemble those of oligonucleotide **9** as shown in Fig. 4b. Thus, the introduction of one propynylated nucleoside residue does not cause significant changes in the CD spectra and does not effect i-motif formation.

Next, the oligonucleotide **12** was studied which contains a complete run of propynylated dC-residues (**2**) in place of dC. In this case, a disulfide chain was linked to the oligonucleotide suitable for the immobilization on gold nanoparticles after reduction. This oligonucleotide was incubated at the same pH value (pH = 5) as used for the experiments described above. Although the incubation time was extended to 20 days, no characteristic spectra indicative for the i-motif structure could be detected (Fig. 4c). The spectra were identical to those obtained for the random state at pH 8 (data not shown). Due to the lower pK_a value of 5-propynyl-2′-deoxycytidine (**2**; pK_a = 3.3) compared to the parent 2′-deoxycytidine (**1**; pK_a = 4.5) we reasoned that oligonucleotides incorporating the propynyl derivative **2** require lower pH values for i-motif formation. Thus, it seemed to be essential to use more acidic conditions to achieve the formation of the hemiprotonated 5-propynyl-2′-deoxycytosine base pair as indicated by motif I (Fig. 1e). Consequently, the propynylated oligonucleotide **12** was incubated at pH = 3.5. Within several hours the CD spectra showed the pattern indicative of i-motif formation of the oligomer **12** (Fig. 4d). It should be noted that the CD spectra of oligonucleotides incorporating 2′-deoxy-5-propynylcytidine residues are significantly different to those obtained from oligonucleotides incorporating unmodified dC residues. This is not surprising, as even 2′-deoxy-5-propynylcytidine (**2**) shows UV spectra significantly different from those of 2′-deoxycytidine (Fig. 3), causing the changes in the CD spectra (Fig. 5).[36] The strong Cotton effects near 265 nm (negative), and around 240 nm and 320 nm (positive) observed for the i-motif assembly of **12** (10–30 °C) change significantly at elevated temperature due to the disassembly of the i-motif. At higher temperatures (**12**: 40–70 °C) the negative lobe becomes indistinct and the spectra adopt the shape of those measured at pH 5 or pH 8. Next, the CD spectra obtained from 5′-d(T-T-C-C-C-C-T-T) (**8**) and its fully propynylated derivative **11** were compared, as shown in Fig. 4a. At pH 5, the CD spectra of oligomer **8** show the characteristic signature of the i-motif. Consistent with the results obtained from oligomer **12**, no i-motif structure could be detected for oligomer **11** at pH 5 (Fig. 4a). However, the incubation of the propynylated oligonucleotide **11** at pH 3.5 led to i-motif formation as proved by the CD spectra (data not shown). Nevertheless, the i-motif formation of **11** required a longer incubation time (5 days) and led to a low content of i-motif assemblies as indicated by the CD spectra (data not shown).

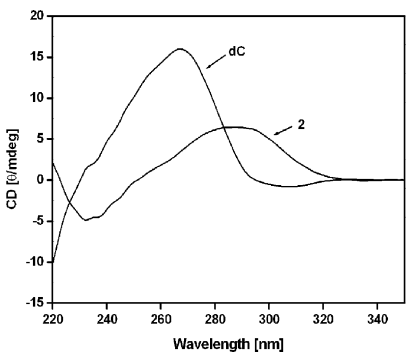

Fig. 5 CD spectra of the nucleosides dC and **2** measured in a 0.3 M NaCl, 10 mM phosphate buffer solution at pH 7 and at a concentration of 1.4 × 10^{-4} M.

Earlier, the multimer stoichiometry of cytosine-rich oligonucleotides was analyzed by non-denaturing gel electrophoresis as well as by gel-filtration chromatography.[15,37–38] However, ion-exchange chromatography can also be used to separate single-stranded oligonucleotides from their multimer assemblies due to a change in the negative charges of the four-stranded complex. This phenomenon has already been used to analyze the formation of dG-quartets and isoG$_d$-oligonucleotide assemblies.[39–40] Under acidic conditions (pH 5) the single-stranded oligonucleotide **9** can be well separated from the tetrameric structure (Fig. 6a). The fast migrating peak (t_R = 13 min) was assigned to the single strand while the slower one (t_R = 19 min) represents the tetrameric assembly. This is a direct consequence of the large increase of negative charges of the i-motif assembly compared to the single-stranded species. When the eluting buffer was changed from pH 5 to pH 8 the tetrameric i-motif structure was not detected and only the single-stranded species appeared with a retention time (t_R = 14 min) almost identical to that obtained for the fast-migrating peak detected at pH 5 (Fig. 6d). The same experiment was performed with oligonucleotide **10** incorporating one residue of the propynylated nucleoside **2**. This led to a similar result (single strand of **10**: t_R = 12 min; multi-stranded **10** assembly: t_R = 19 min). The mixture of the oligonucleotides **9** and **10** carrying the same number of charges shows an almost identical chromatographic behaviour, indicating that the propynyl group has a minor influence on the mobility. The fully propynylated oligonucleotide **12** chromatographed at pH 5 shows a strong peak formed by the single strand (t_R = 15 min) and only a small peak for the i-motif assembly (t_R = 20 min). This is indicative for the restricted i-motif formation caused by the low pK_a value of protonation for compound **2** (pK_a = 3.3).

Next, temperature-dependent melting studies were performed to evaluate the stability of the i-motif structures formed by the non-branched oligonucleotides **7**–**12** (Table 3). As 5-propynylated nucleosides have been shown to increase duplex and triplex stability significantly,[26–29] the effect of the propynyl group on the i-motif structures was now investigated and compared to

Table 3 T_m values (in °C) of i-motif-forming non-branched oligonucleotides[a]

Oligonucleotide	pH 3.5	pH 5
5′-d(C-C-C-C-C)[19,20] (**7**)	—[b]	30
5′-d(T-T-C-C-C-C-T-T) (**8**)	—[b]	47
5′-d(T-T-C-C-C-C-C-C-T-T) (**9**)	—[b]	21/59[d]
5′-d(T-T-C-C-C-**2**-C-C-T-T) (**10**)	45	<23/55[d]
5′-d(T-T-**2**-**2**-**2**-**2**-T-T) (**11**)	28	—[c]
5′-d(T-T-**2**-**2**-**2**-**2**-**2**-**2**-T-T)-$(CH_2)_3$-S-S-$(CH_2)_3$-OH (**12**)	33/65[d]	—[c]

[a] Measured at 235 nm as heating curves (0.5 °C min^{-1}) in 0.3 M NaCl, 10 mM phosphate buffer with 12.9 μM single-strand concentration. [b] Not measured. [c] No i-motif formation observed. [d] Biphasic melting.

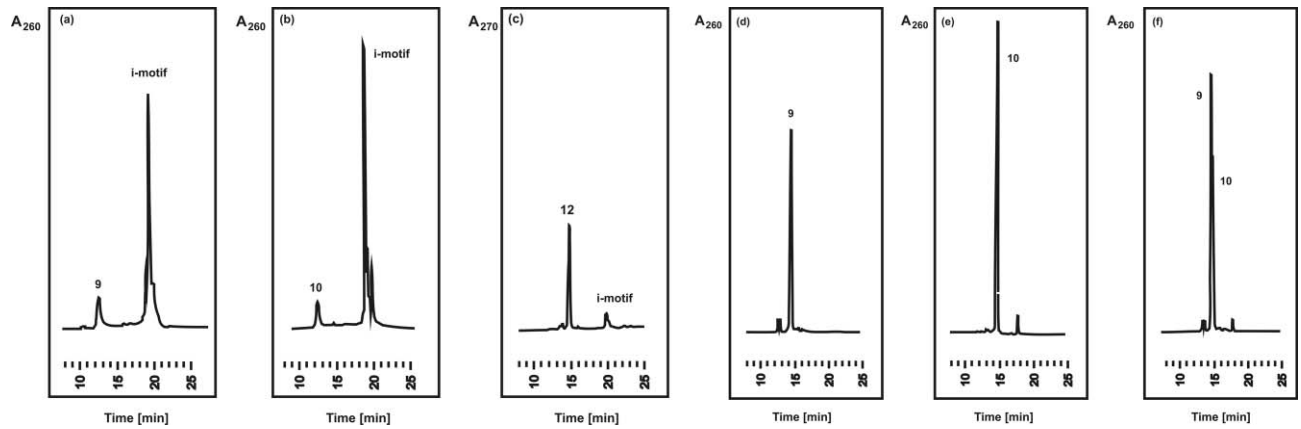

Fig. 6 Ion-exchange HPLC elution profiles with detection at 260 nm; for compound **12** at 270 nm: (a) 5′-d(T-T-C-C-C-C-C-C-T-T) (**9**), (b) 5′-d(T-T-C-C-C-**2**-C-C-T-T) (**10**) and (c) d[(T-T-**2**-**2**-**2**-**2**-**2**-**2**-T-T)-$(CH_2)_3$-S-S-$(CH_2)_3$-OH] (**12**) with an elution buffer system at pH 5; (d) oligonucleotide **9**, (e) oligonucleotide **10** and (f) a mixture of **9** and **10** with an elution buffer system at pH 8. The ion-exchange chromatography was performed on a 4 × 50 mm NucleoPac PA-100 column using the following buffer system: (A) 25 mM Tris-HCl containing 1 mM EDTA and 10% MeCN; (B) 25 mM Tris-HCl containing 1 mM EDTA, 1 M NaCl, and 10% MeCN. Eluting gradient: 3 min 20% B in A, 30 min 20–80% B in A.

corresponding unmodified species. At first, the oligonucleotides **7–9** containing consecutive dC residues were incubated in 0.3 M NaCl, 10 mM phosphate buffer at pH 5 for several days, and the melting experiments were performed in the heating mode (dissociation of the i-motif) with a temperature increase of 0.5 °C min^{-1}. The melting of i-motif structures was detected by a hyperchromic transition at 235 nm and a hypochromic transition at 295 nm. The T_m value of the i-motif formed by dC_5 (**7**)[19,20] at pH 5 was 30 °C (0.3 M NaCl, 10 mM phosphate buffer). Although the i-motif formed by oligonucleotide 5′-d(T-T-C-C-C-C-T-T) (**8**) contains only four dC residues, the T_m value of 47 °C is significantly higher than that of the the i-motif of **7**. This T_m value for **8** is consistent with that obtained from the temperature-dependent CD measurement (Fig. 4a). It seems that the additional dT residues at the 3′- and 5′-ends have a stabilizing effect on the i-motif structure.

The i-motif assembly of 5′-d(T-T-C-C-C-C-C-C-T-T) (**9**) containing six dC residues reveals a biphasic melting with a low and a high T_m value at pH 5. The higher melting temperature of **9** (T_m = 59 °C) is consistent with the value previously reported for the i-motif structure formed by the comparable sequence 5′-d(T-C-C-C-C-C-C) (T_m = 59 °C) measured in 50 mM sodium citrate, pH 4.6 within the same concentration range (11.5 μM).[41] As this T_m value was assigned to i-motif melting, it can be concluded that the higher T_m value of **9** corresponds to the melting of the fully paired tetrameric i-motif structure (Fig. 1b) whereas the lower T_m value might be caused by the formation of a hemi-protonated duplex (Fig. 1a). Moreover, the CD spectra of **9** obtained from temperature-dependent CD measurements reveal a significant change in their shape between 55 °C and 65 °C due to the disassembly of the i-motif (data not shown). These findings are also supported by melting experiments performed in the cooling mode (75 °C → 15 °C) or with only a few hours of incubation time resulting only in a low T_m value. This phenomenon was also reported for other i-motifs.[42–43] Interestingly, the same biphasic melting phenomenon was also observed for the i-motifs formed by the modified oligonucleotides 5′-d(T-T-C-C-C-**2**-C-C-T-T) (**10**) and 5′-d(T-T-**2**-**2**-**2**-**2**-**2**-**2**-T-T)-$(CH_2)_3$-S-S-$(CH_2)_3$-OH (**12**) incubated in 0.3 M NaCl, 10 mM phosphate buffer (pH 5 for **10** and pH 3.5 for **12**). The introduction of one modified residue **2** instead of dC leads to a destabilization of the i-motif assembly of **10** by 5 °C at pH 5 (**10**: T_m = 55 °C), whereas at pH 3.5 the complete replacement of the dC residues by **2** causes a strong stabilization of the i-motif structure of 6 °C (**12**: T_m = 65 °C). The i-motif formed by oligonucleotide **11** employing four 2′-deoxy-5-propynylcytosine residues (**2**) is significantly less stable at pH 3.5 (T_m = 28 °C). According to the low number of 5-propynyl-dC residues it is likely that the T_m value of 28 °C represents the melting of a mixture (hemi-protonated duplex and i-motif).

5. i-Motif formation of branched oligonucleotides

Several structural features make cytosine-rich branched oligonucleotides highly attractive candidates for i-motif formation. The group of Damha *et al.* synthesized "V"-shaped branched oligonucleotides employing a riboadenosine branching point connecting the chains *via* the 2′,3′-hydroxyl groups.[19–20] The cytosine-rich oligonucleotide chains are of equal strand polarity and are forced into close proximity thereby facilitating parallel cytosine base pairing. The molecularity of this process is reduced from a four-fold assembly to a two-fold assembly leading to a favourable entropy change during i-motif formation. However, the introduction of a branching unit decreases the conformational freedom of the oligonucleotide strands. We decided to utilize the concept of branched structures to increase the stability of i-motifs. For this, the modified branched oligonucleotides **17** and **18** incorporating 2′-deoxy-5-propynylcytidine residues were synthesized and their stability was compared to the unmodified branched oligonucleotides **13–16** (for sequences see Table 4). As a branching unit, a commercially available flexible linker originally reported by Shchepinov[44] was used. Other branching units have already been used for various purposes by the groups of Damha[19–20,45] and Chattopadhyaya[46–47] as well as by our group.[48] Table 4 displays branched oligonucleotides which are used in this study and shows the corresponding masses determined by MALDI-TOF mass spectrometry.

Table 4 Branched oligonucleotides **13–18** and their molecular masses determined by MALDI-TOF mass spectrometry

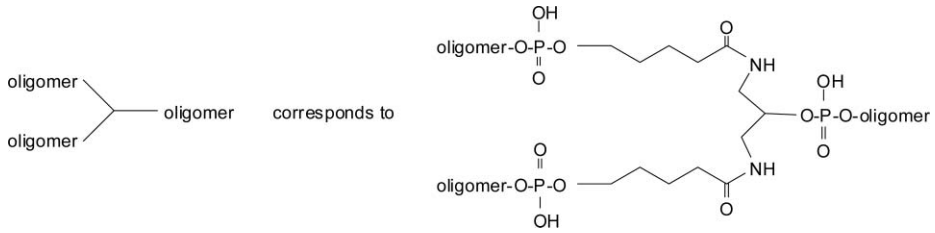

Branched oligonucleotides	[M + H]$^+$ (Da) Calc.	Found
5'-d(C-C-C-C-T-T) 5'-d(C-C-C-C-T-T) — 5'-d(T-T-T-T)-3' (**13**)	5038	5038
5'-d(T-T-C-C-C-C-T-T) 5'-d(T-T-C-C-C-C-T-T) — 5'-d(T-T-T-T)-3' (**14**)	6255	6255
5'-d(C-C-C-C-C-C-T-T) 5'-d(C-C-C-C-C-C-T-T) — 5'-d(T-T-T-T)-3' (**15**)	6194	6195
5'-d(T-T-C-C-C-C-C-C-T-T) 5'-d(T-T-C-C-C-C-C-C-T-T) — 5'-d[(T-T-T-T)-$(CH_2)_3$-S-S-$(CH_2)_3$-OH]-3' (**16**)	7655	7655
5'-d(**2-2-2-2-2-2**-T-T) 5'-d(**2-2-2-2-2-2**-T-T) — 5'-d(T-T-T-T)-3' (**17**)	6652	6651
5'-d(T-T-**2-2-2-2-2-2**-T-T) 5'-d(T-T-**2-2-2-2-2-2**-T-T) — 5'-d[(T-T-T-T)-$(CH_2)_3$-S-S-$(CH_2)_3$-OH]-3' (**18**)	8112	8113

Temperature-dependent CD measurements of the oligonucleotides **13–18** performed in the heating mode confirmed the formation of i-motif structures under acidic conditions in all cases (0.3 M NaCl, 10 mM phosphate buffer, pH 5 or pH 3.5). From the temperature-dependent spectra of the dC-containing oligonucleotides **13–16** (Fig. 7 and Fig. 8) the formation of the i-motif assembly was deduced by the large positive Cotton effect observed around 280 nm and the negative lobe at 260 nm (Fig. 7a). The spectra changed upon heating, resulting in the final curves of the non-assembled strands, which look almost identical to those measured at pH 8. A similar phenomenon was observed for the propynylated branched oligonucleotides **17** and **18**. Also, their CD spectra changed significantly during the temperature increase; however, due to spectral differences of the UV-spectra of dC and compound **2** the temperature-induced changes of the Cotton effects are now shifted to longer wavelengths (Fig. 7b: 320 nm, 240 nm, 280 nm).

Two additional points have to be mentioned. (i) The i-motif formation of the propynylated oligonucleotides formed within a branched structure occurs even at pH 5, which is distinctly higher than the pK_a value of the monomeric nucleoside **2**. This phenomenon is not observed with non-branched propynylated oligonucleotides incorporating a 5-propynyl-dC-rich region. This might be explained by local pK_a changes of protonation between individual strands and branched structures. Such an observation has already been reported for branched and non-branched i-motifs containing consecutive dC-moieties.[19] Furthermore, the branching residue clamps two strands together. Accordingly, a separation of the i-motif formed by the branched strands is retarded in comparison to the non-branched i-motif even when the same number of dC-residues are protonated. (ii) The propynylated branched oligonucleotides **17** and **18** form extremely stable i-motifs (see next paragraph). Thus, the temperature-dependent CD spectral changes obtained for compound **17** at pH 3.5 do not lead to the fully disassembled motifs thereby not showing the final hypsochromic CD change (Fig. 7b) as observed for the corresponding oligonucleotide **15** containing unmodified dC residues (Fig. 7a). A complete change occurs at pH 5 due to the less stable i-motif structure (Fig. 7c). These results clearly show that i-motif formation is not only possible for branched oligonucleotides incorporating the canonical 2′-deoxycytidine constituent, but also for branched oligonucleotides incorporating consecutive runs of the 2′-deoxy-5-propynylcytidine (**2**) carrying a bulky side chain in the 5-position. The introduction of a branching residue leads to a stabilization of the modified branched oligonucleotides **17** and **18** even at pH values significantly higher than the pK_a value of the monomeric nucleoside (pH 5 *vs.* pH 3.5).

Next, ion-exchange chromatography was performed with the branched oligonucleotides **13–18** as described for the non-branched oligonucleotides (Fig. 9). At pH 5 the elution profiles

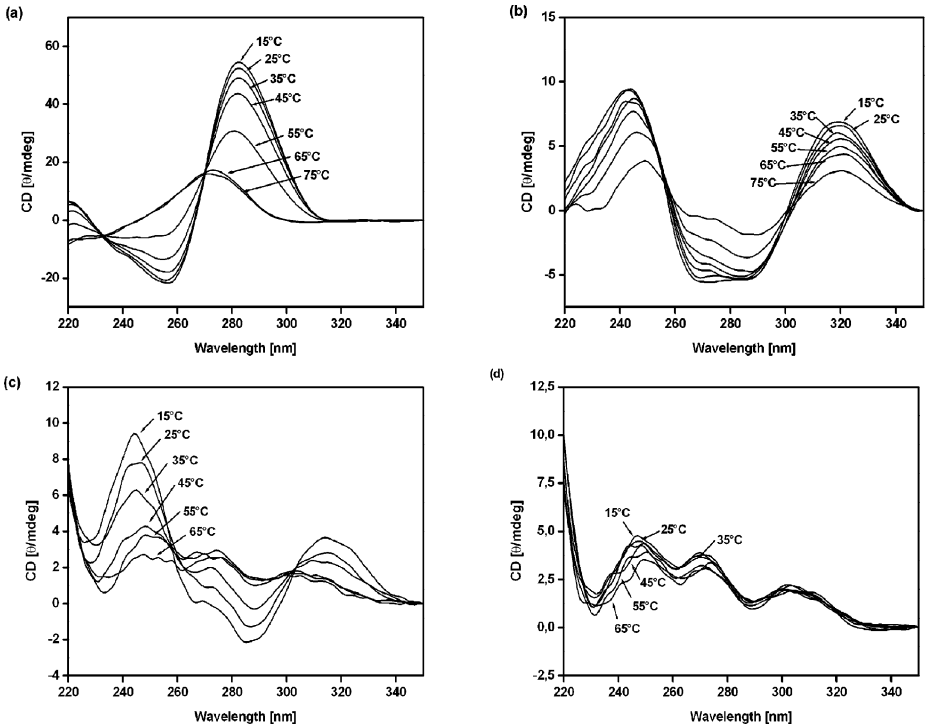

Fig. 7 CD spectra of the tetrameric i-motif assembly formed by two branched units of **15** measured in 0.3 M NaCl, 10 mM sodium phosphate buffer, pH 5 (a) and the tetrameric i-motif assembly formed by two branched units of **17** measured in 0.3 M NaCl, 10 mM sodium phosphate buffer at pH 3.5 (b) and at pH 5 (c); the monomeric species of **17** at pH 8 (d).

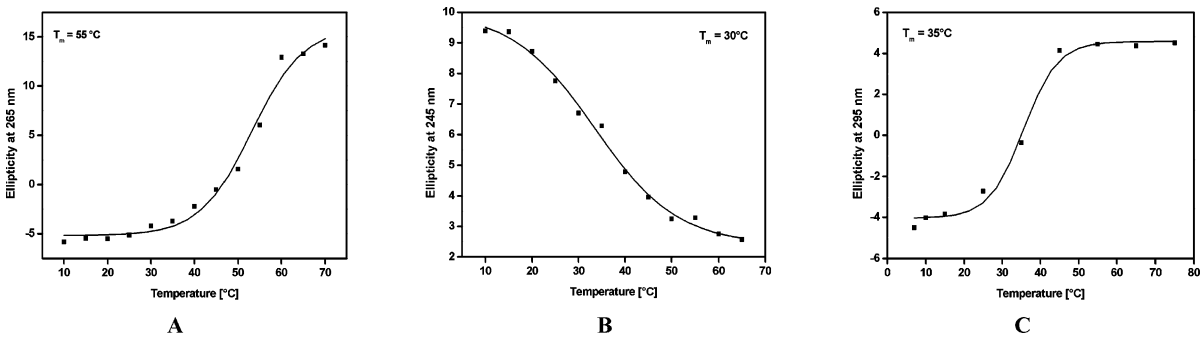

Fig. 8 T_m values of the branched oligonucleotides **15** (A), **17** (B) and **18** (C) determined by temperature-dependent CD measurements in 0.3 M NaCl, 10 mM phosphate buffer at pH 5.

of compound **15** and its propynylated derivative **17** show a peak each with a similar retention time around 20 min (**15**: $t_R = 20$ min; **17**: $t_R = 19$ min; Fig. 9a,b). Nevertheless, in both cases the peak is significantly broadened, indicating the elution of an aggregate. This finding is supported by comparison with the elution profile of the non-branched oligonucleotide **9** obtained under the same conditions (pH 5). As oligonucleotides **9**, **15** and **17** have the same overall charge while forming the i-motif (per i-motif structure: 40 negative charges for the phosphate groups *vs.* 12 positive charges of the hemiprotonated cytosine base pairs), very similar retention times can be expected. Indeed, the elution profile of **9** shows the migration of the i-motif assembly at $t_R = 19$ min (Fig. 6a). The branched oligonucleotides show additional small peaks at higher retention times ($t_R = 22$ min and $t_R = 24$ min) which are not found in the profiles of the non-branched oligonucleotides. These peaks probably refer to higher aggregates. When the eluting buffer was changed from pH 5 to pH 8 only the single-stranded species appeared, showing a strong peak with a retention time of $t_R = 21$ min for **15** and $t_R = 20$ min for **17** (Fig. 9d,e). However, the injection of a mixture of both oligonucleotides carrying the same number of charges revealed that the completely propynylated compound **17** migrates only slightly faster than the unmodified oligonucleotide **15** (Fig. 9f).

Next, T_m studies were performed with the oligonucleotides **13**–**18** (Table 5). The melting refers to the dissociation of the i-motif structures while association of the i-motif structures occurs upon cooling (rate of 0.5 °C min^{-1}). In contrast to the non-branched oligonucleotides, at pH 5 dissociation of the i-motifs formed by the unmodified branched oligonucleotides **13**–**16** followed by their re-association could be detected by cycling the temperature

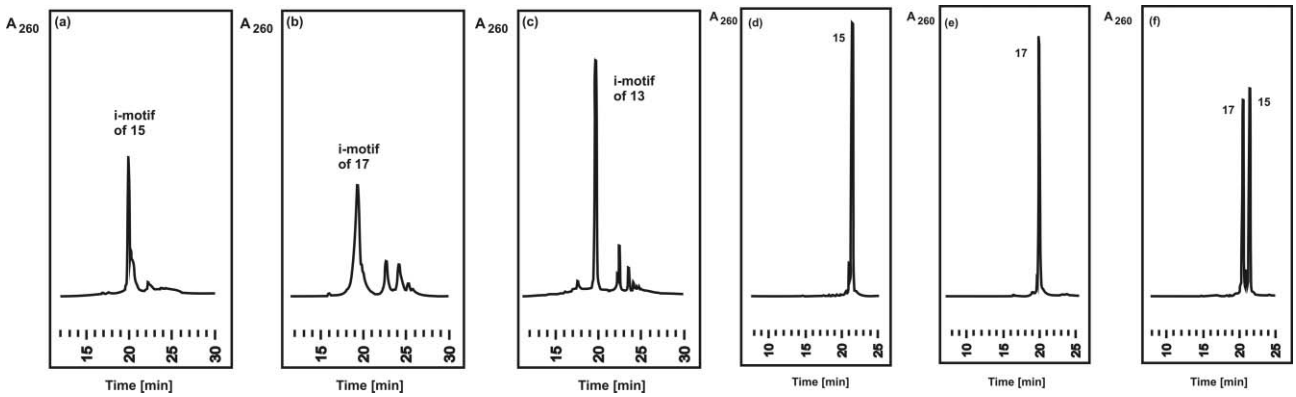

Fig. 9 Elution profiles of ion-exchange HPLC with detection at 260 nm. (a–c): Elution buffer system at pH 5: (a) branched oligonucleotide **15**, (b) branched oligonucleotide **17** incorporating **2** and (c) branched oligonucleotide **13**. (d–f): Elution buffer system at pH 8: (d) branched oligonucleotide **15**, (e) branched oligonucleotide **17** and (f) mixture of the branched oligonucleotides **15** and **17**. The ion-exchange chromatography was performed on a 4 × 50 mm NucleoPac PA-100 column using the following buffer system: (A) 25 mM Tris-HCl containing 1 mM EDTA and 10% MeCN; (B) 25 mM Tris-HCl containing 1 mM EDTA, 1 M NaCl, and 10% MeCN. Eluting gradient: 3 min 20% B in A, 30 min 20–80% B in A.

Table 5 T_m values (in °C) of i-motif-forming branched oligonucleotides[a]

Branched oligonucleotides	pH 3.5	pH 5
5'-d(C-C-C-C-C-T-T) 5'-d(C-C-C-C-C-T-T) — 5'-d(T-T-T-T)-3' (**13**)	—[b]	37
5'-d(T-T-C-C-C-C-C-T-T) 5'-d(T-T-C-C-C-C-C-T-T) — 5'-d(T-T-T-T)-3' (**14**)	—[b]	49
5'-d(C-C-C-C-C-C-C-T-T) 5'-d(C-C-C-C-C-C-C-T-T) — 5'-d(T-T-T-T)-3' (**15**)	31	57
5'-d(T-T-C-C-C-C-C-C-C-T-T) 5'-d(T-T-C-C-C-C-C-C-C-T-T) — 5'-d[(T-T-T-T)-$(CH_2)_3$-S-S-$(CH_2)_3$-OH]-3' (**16**)	—[b]	40
5'-d(**2-2-2-2-2-2**-T-T) 5'-d(**2-2-2-2-2-2**-T-T) — 5'-d(T-T-T-T)-3' (**17**)	77	37
5'-d(T-T-**2-2-2-2-2-2**-T-T) 5'-d(T-T-**2-2-2-2-2-2**-T-T) — 5'-d[(T-T-T-T)-$(CH_2)_3$-S-S-$(CH_2)_3$-OH]-3' (**18**)	70	39

[a] Measured at 235 nm as heating curves (0.5 °C min^{-1}) in 0.3 M NaCl, 10 mM phosphate buffer with 4.3 μM single-strand concentration. [b] Not measured.

(heating/cooling rate: 0.5 °C min^{-1}). As indicated by Fig. 10a, a hysteresis can be observed, which is indicative for the slower kinetics of the i-motif formation. Nevertheless, i-motif formation of branched oligonucleotides is faster compared to i-motif formation of the non-branched oligonucleotides, as indicated by the immediate formation of the branched i-motif structures; the assembly of non-branched oligonucleotides into i-motif structures required several hours. The non-branched oligonucleotides did not re-associate at this cooling rate.

Interestingly, the branched oligonucleotides **17** and **18** incorporating **2** instead of dC also could not re-associate at this cooling rate (Fig. 10b). This phenomenon is consistent with an arrangement process of the modified branched oligonucleotides into the final i-motif structure whereas the formation of a hemi-protonated duplex should occur much faster due to rapid protonation and deprotonation. Moreover, the T_m studies of the branched oligonucleotides (**13–18**) always revealed a monophasic transition. A biphasic transition as found for the non-branched oligonucleotides **9**, **10** or **12** was never detected.

Upon heating, a T_m value of 37 °C was detected at pH 5 for the i-motif of the branched oligonucleotide **13**. Increasing the numbers of dC residues from four to six leads to a significant stabilization of the i-motif structure (**15**: T_m = 57 °C). A strong influence on the i-motif stability is also observed by the 5′-dT residues. For the shorter oligonucleotide **14** a strong stabilization could be detected (37 °C for **13** *vs.* 49 °C for **14**) whereas for the longer oligonucleotide **16** a severe destabilization was found (57 °C for **15** *vs.* 40 °C for **16**). The branched oligonucleotides **17** and **18**

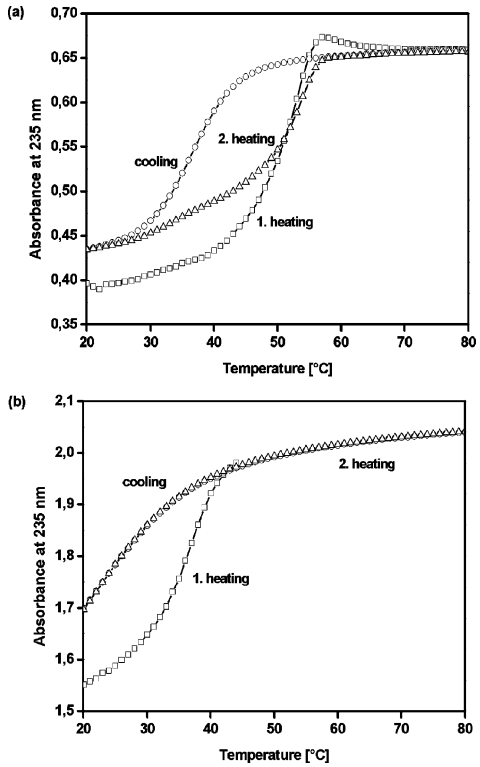

Fig. 10 Dissociation and association of the i-motif structure formed by the branched oligonucleotides **15** (a) and **17** (b). □ First heating, 20 °C → 80 °C; ○ Cooling, 80 °C → 20 °C; △ Second heating, 20 °C → 80 °C (heating/cooling rate: 0.5 °C min^{-1}).

incorporating **2** instead of dC form i-motif structures at pH 3.5 which are significantly more stable than their parent unmodified assemblies (pH 5) (70 °C for **18** *vs.* 40 °C for **16**, and 77 °C for **17** *vs.* 57 °C for **15**). Thus, even under non-optimal pH conditions (pH = 5) **17** and **18** form stable i-motif structures as indicated by their T_m values (37 °C for **17** and 39 °C for **18**). However, it has to be kept in mind that the most stable i-motif structures are formed when a hemi-protonated base pair is present. Below and above this pK_a value the i-motif structure is destabilized. This is underlined by the fact that for the non-propynylated oligonucleotide **15** a T_m value of 57 °C is observed at pH 5 which decreases to 31 °C at pH 3.5. The situation is reversed in the case of the propynylated oligonucleotide **17**. Here, the more stable i-motif is formed at pH 3.5 (T_m = 77 °C), being less stable at pH 5 (T_m = 37 °C). The results show that the incorporation of multiple propynyl groups at the 5-position of the 2′-deoxycytidine moieties has a stabilizing effect on the i-motif structure. The stabilization is much more pronounced for the i-motifs formed by branched oligonucleotides compared to the i-motif assemblies of non-branched oligonucleotides.

6. Preparation and properties of DNA–gold nanoparticle conjugates

To visualize i-motif formation of oligonucleotides incorporating consecutive 2′-deoxy-5-propynylcytidine residues (**2**) bound to gold nanoparticles, the 5′-thiol-modified oligonucleotide **19** was prepared and conjugated to the surface of the nanoparticles

Table 6 Gold nanoparticles of 15 nm diameter functionalized with an arbitrary number of oligonucleotides

DNA–gold nanoparticle conjugates
5′-d{[Trityl-S-$(CH_2)_6$-O(PO_2H)O]-T-T-**2-2-2-2-2-2**-T-T} (**19**)
5′-●-[S-$(CH_2)_6$-O(PO_2H)O-d(T-T-**2-2-2-2-2-2**-T-T)]$_n$ (**20**)
5′-d{[Trityl-S–$(CH_2)_6$–O(PO_2H)O]-(A-G-T-A-T-T-G-A-C-C-T-A)$_2$} (**21**)
5′-●-[S-$(CH_2)_6$-O(PO_2H)O-d(A-G-T-A-T-T-G-A-C-C-T-A)$_2$]$_n$ (**22**)
● = 15 nm diameter gold nanoparticle

(Table 6). For this, a 15 nm diameter gold nanoparticle solution was prepared from a $HAuCl_4$ solution by citrate reduction according to the procedure of Turkevich.[35,49] The UV/VIS spectrum of the unmodified gold nanoparticle solution shows the characteristic plasmon resonance at 520 nm (Fig. 11A-a). The immobilization of **19** on the 15 nm gold nanoparticles was performed as described recently.[50] Prior to functionalization, the pH of the gold nanoparticle solution was raised from pH 5.5 to pH 9.5 avoiding i-motif formation of the non-bound oligonucleotides. The DNA-modified gold nanoparticle sample **20** was prepared by mixing the alkaline gold nanoparticle solution (6.4 ml) with the oligonucleotide solution of **19** (3.5 ml) obtained after trityl group removal and purification.[35,50] The coupling reaction was performed at slightly elevated temperature. The resulting DNA–gold conjugate **20** (Table 6) shows the expected plasmon resonance at around 525 nm under alkaline conditions (Fig. 11A-b), indicating a non-aggregated state. The number of oligonucleotides immobilized on each individual gold nanoparticle is arbitrary.

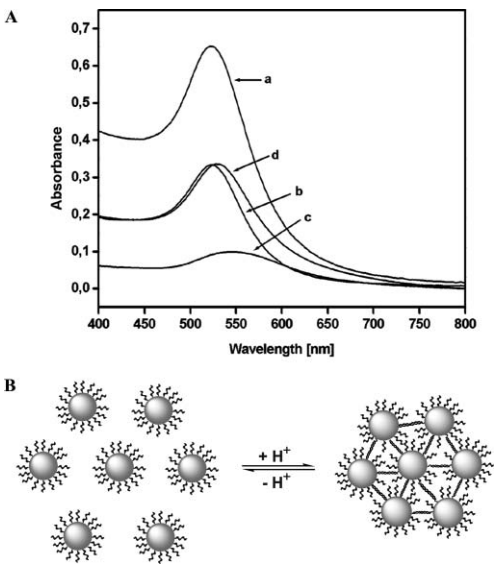

Fig. 11 A: UV/VIS spectra of (a) the alkaline solution (pH = 9) of 15 nm diameter gold nanoparticles; (b) the DNA–gold nanoparticle conjugate **20** measured in 0.1 M NaCl, 10 mM phosphate buffer solution at pH = 8.0; (c) **20** measured in 0.1 M NaCl, 10 mM phosphate buffer solution at pH = 5 after i-motif formation and (d) the DNA–gold nanoparticle conjugate **22** measured in 0.1 M NaCl, 10 mM phosphate buffer solution at pH = 5.0. B: Representation of the reversible aggregation process of DNA–gold nanoparticles conjugates forming i-motif assemblies.

Earlier, Mirkin and Alivisatos developed a colorimetric assay based on the reversible aggregation of DNA-modified gold

nanoparticles followed by the colour change of the gold nanoparticle solution from red to blue.[51–55] Our laboratory was the first to show that gold nanoparticle aggregation can also be achieved by other unusual DNA assembly structures such as the dG-quartet and the i-motif.[50,56] We reported on the ability of cytosine-rich DNA–gold nanoparticle conjugates to respond to pH changes within a narrow range due to the assembly and disassembly of i-motif structures.[50] Above pH 6.5 these DNA-modified gold nanoparticles are disperse in solution, corresponding to the disassembly of the i-motif. The i-motif structure is formed at pH values below 5.5, leading to the assembly of the DNA–gold nanoparticles. Accordingly, it was expected that a similar principle should also be valid for the DNA–gold nanoparticle conjugate **20** incorporating consecutive 2′-deoxy-5-propynylcytosine residues. However, on the surface of the gold nanoparticles the immobilized oligonucleotides are forced into close proximity, leading to a steric situation similar to that of branched oligonucleotides with parallel-stranded oligonucleotide chains. As the branched oligonucleotide **18** forms an i-motif structure even at non-optimal pH values (pH = 5) that are distinctly higher than the pK_a value of the 5-propynyl-2′-deoxycytidine nucleoside (**2**), it can be expected that the i-motif formation of DNA–gold nanoparticle conjugates incorporating multiple residues of nucleoside **2** should be possible at pH 5. Consequently, the DNA–gold nanoparticle conjugate **20** was incubated in phosphate buffer at pH 5. Within 24 h, aggregation of the DNA-modified gold nanoparticles occurred, which was indicated by a red shift of the plasmon resonance from 525 nm to 545 nm accompanied by a colour change of the solution from red to blue (Fig. 11A-c). A DNA–gold nanoparticle conjugate of random nucleobase composition (**22**) stayed red under the same conditions and no shift of the plasmon resonance band was observed (Fig. 11A-d).

The aggregation of the DNA–gold nanoparticle conjugates **20** can be attributed to i-motif formation of immobilized oligonucleotides derived from different gold nanoparticles (Fig. 12c). The colour change from red to blue as a consequence of irreversible particle growth can be excluded. Upon i-motif formation, the total amount of negative charges per unit is sufficient to cause electrostatic repulsion of the gold nanoparticles. Even the formation of hemiprotonated duplexes of oligonucleotides which are not involved in i-motif formation leads to a total of 8 negative charges per unit (Fig. 12b). This corresponds to DNA–gold nanoparticles modified with octamers. The high stability of the DNA–gold nanoparticles forming i-motif structures can be attributed to a high local concentration of oligonucleotides on the surface of the particles. In the case of standard duplex formation of DNA–gold nanoparticles, the higher local surface concentration on the particle surfaces leads to significant higher T_m values and ΔG° values compared to the free oligonucleotides.[57]

Conclusion and outlook

Cytosine-rich non-branched and branched oligonucleotides that are able to form i-motif structures under slightly acidic conditions were synthesized. The replacement of 2′-deoxycytidine by 2′-deoxy-5-propynylcytidine (**2**) caused the formation of i-motifs. These i-motif assemblies were formed by four individual strands, branched oligonucleotides or DNA– gold nanoparticle conjugates. This was proved by temperature-dependent CD measurements and UV measurements, as well as by ion-exchange chromatography. However, due to the lower pK_a value of nucleoside **2** compared to dC, stronger acidic conditions were required for i-motif formation of the non-branched oligonucleotides (pH 3.5). A strong stabilization of the modified i-motif structures at pH 3.5 was observed when branching residues linking two oligonucleotide strands in a parallel orientation were introduced. Thus, i-motif formation of the modified branched oligonucleotides and of the DNA–gold nanoparticle conjugates was also possible at non-optimal pH values (pH 5). It can be anticipated that other side chains such as octa-1,7-diynyl should also be accepted at this position.[58] The introduction of these linkers into i-motif structures allows the attachment of various reporter groups by the Huisgen–Meldal–Sharpless [2 + 3] cycloaddition ("click chemistry"),[59,60] as well as formation of large oligonucleotide assemblies *via* cross-linked nucleobases that are part of the i-motif device.

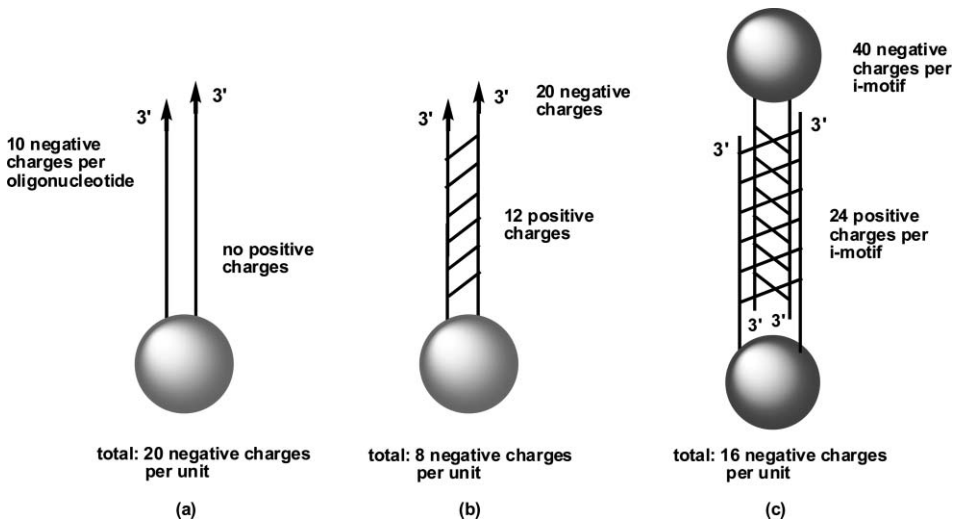

Fig. 12 Schematic representation of modified gold nanoparticles. (a) Single-stranded oligonucleotides conjugated to gold nanoparticles, (b) formation of hemiprotonated duplexes on the surface of gold nanoparticles and (c) aggregation of DNA–gold nanoparticles due to i-motif formation.

Experimental

General

All chemicals were purchased from Aldrich, Sigma, or Fluka (Sigma-Aldrich Chemie GmbH, Deisenhofen, Germany). Solvents were of laboratory grade. TLC: aluminium sheets, silica gel 60 F_{254}, 0.2 mm layer (VWR International, Darmstadt, Germany). Column flash chromatography (FC): silica gel 60 (VWR International, Darmstadt, Germany) at 0.4 bar; sample collection with an UltroRac II fractions collector (LKB Instruments, Sweden). The 5′-sulfanyl modifier 6-[(triphenylmethyl)sulfanyl]hexyl(2-cyanoethyl) *N*,*N*-diisopropylphosphoramidite and the 3′-sulfanyl modifier 1-*O*-dimethoxytrityl propyl disulfide 1′-succinyl-CPG were obtained from Glen Research (Virginia, USA). UV/VIS spectra were recorded with U-3000 and U-3200 spectrophotometers (Hitachi, Tokyo, Japan); λ_{max} (ε) in nm. CD spectra were measured as accumulations of three scans with a Jasco 600 (Jasco, Japan) spectropolarimeter with a thermostatically (Lauda RCS-6 bath) controlled 1 cm quartz cuvette. NMR spectra: Avance-250 or AMX-500 spectrometers (Bruker, Karlsruhe, Germany), at 250.13 MHz for ^{1}H and ^{13}C; δ in ppm relative to Me_4Si as internal standard, *J* values in Hz. Elemental analyses were performed by Mikroanalytisches Laboratorium Beller (Göttingen, Germany). The melting temperatures were measured with Cary-1/3 UV/VIS and Cary 100 Bio spectrophotometers (Varian, Australia) equipped with a Cary thermoelectrical controller. The temperature was measured continuously in the reference cell with a Pt-100 resistor.

Synthesis, purification and characterization of the oligonucleotides

The oligonucleotides **10**–**19** and **21** were synthesized in an automated DNA synthesizer (ABI 392, Applied Biosystems, Weiterstadt, Germany) on a 1 μmol scale employing standard phosphoramidites as well as the phosphoramidite **3b**. For the 3′-thiol modification of **12**, **16** and **18** a 3′-thiol-modifier, C3 S–S CPG (Glen Research, US), was used, and for the 5′-thiol modification of **19** and **21** a 5′-thiol-modifier, C6-phosphoramidite (Glen Research, US), was employed. The syntheses of the 3′- and 5′-thiol-modified oligonucleotides were carried out according to the standard procedure for solid-phase synthesis of oligonucleotides.[34] The purification of the 3′-thiol-modified oligonucleotides was performed by reversed-phase HPLC (RP-18) in the DMT-on modus with the following solvent gradient system [A: 0.1 M (Et_3NH)OAc (pH 7.0)–MeCN 95 : 5; B: MeCN]: 3 min, 20% B in A, 12 min, 20–50% B in A and 25 min, 20% B in A with a flow rate of 1.0 ml min^{-1}. The solutions were dried and treated with 80% CH_3COOH (250 μl) for 30 min at r.t. to remove the 4,4′-dimethoxytrityl residues. The acetic acid was evaporated and the detritylated oligonucleotides were precipitated with 1 M NaCl solution (300 μl) and ethanol (1 ml) while cooling. After precipitation the oligonucleotides were lyophilized. The 5′-thiol-modified oligonucleotides **19** and **21** were only purified by reversed-phase HPLC (RP-18) in the DMT-on modus. For the syntheses of the branched oligonucleotides **13–18** employing the phosphoramidite of a dendrimeric branching residue (symmetric doubling modifier, Glen Research, US) the synthetic protocol was modified. The introduction of the dendrimeric branching residue led to the formation of two parallel-stranded oligonucleotide chains. The elongation of the two growing oligonucleotide strands was performed in a parallel way, leading to identical sequences of both strands. For that purpose, double-concentrated solutions (0.2 M instead of 0.1 M) of the regular phosphoramidite building blocks and of **3b** were employed during solid-phase synthesis. Thus, the coupling time for each residue was prolonged during synthesis. The purification was performed as described for the 3′-thiol-modified oligonucleotides. The oligonucleotides **10–18** were characterized after precipitation whereas oligonucleotides **19** and **21** were characterized after HPLC purification in the trityl-on level. The molecular masses were determined by MALDI-TOF with a Biflex-III instrument (Bruker Saxonia, Leipzig, Germany) and 3-hydroxypicolinic acid (3-HPA) as a matrix (Tables 2 and 4). The enzymatic hydrolysis of the oligonucleotides was performed as described by Seela and Becher[61] with snake-venom phosphodiesterase (EC 3.1.15.1, *Crotallus adamanteus*) and alkaline phosphatase (EC 3.1.3.1, *Escherichia coli* from Roche Diagnostics GmbH, Germany) in 0.1 M Tris-HCl buffer (pH 8.9) at 37 °C and was carried out on reversed-phase HPLC (RP-18; gradient: 20 min A; 40 min 0–65% B in A; flow rate: 0.7 ml min^{-1}; A: 0.1 M (Et_3NH)OAc (pH 7.0)–MeCN 95 : 5; B: MeCN). Quantification of the constituents was made on the basis of the peak areas, which were divided by the extinction coefficients of the nucleosides [(ε_{260}): dT 8800, dC 7300, **2** 5200].

Ion-exchange chromatography

Ion-exchange chromatography was performed on a 4 × 50 mm DNA NucleoPac PA-100 column (Dionex, USA) using a Merck Hitachi HPLC apparatus with a pump (L-6200) and a UV/VIS-detector (L-4200) connected with an integrator (D-2000). The oligonucleotide samples were dissolved in 0.3 M NaCl, 10 mM phosphate buffer at pH 5 or pH 8 and stored in a refrigerator at 6 °C for 4–24 h before injection. The oligonucleotides were eluted using the following solvent system: A: 25 mM Tris-HCl containing 1 mM EDTA and 10% MeCN, pH 5 or pH 8; B: 25 mM Tris-HCl containing 1 mM EDTA, 1 M NaCl, and 10% MeCN, pH 5 or pH 8. Eluting gradient: 3 min 20% B in A, 30 min 20–80% B in A. The elution profiles were detected at 260 nm; for oligonucleotide **12** at 270 nm.

Preparation of the DNA-modified gold nanoparticles 19 and 21

The trityl protecting groups of **19** and **21** were removed immediately before modification with the gold nanoparticles, by treatment of the dry oligonucleotide sample with a 50 mM $AgNO_3$ solution (150 μl). A milky suspension was formed which was allowed to stand for 20 min at room temperature. Then, a 10 μg ml^{-1} solution of dithiothreitol (200 μl) was added over 5 min. A yellow precipitate was formed which was removed by centrifugation (14 000 rpm) for 30 min.[35,49–50] Aliquots of the sample were purified on a NAP-10 column (Sephadex G-25 Medium, DNA grade; Amersham Bioscience AB, S-Uppsala; equilibrated with 15 ml of nanopure water). The effluents from 0 to 2.5 ml were collected and the volume was adjusted to 3.5 ml with nanopure H_2O.

The 15 nm gold nanoparticle solution was prepared as reported by Turkevitch and later described by Letsinger and Mirkin.[35,49] Prior to modification, the gold nanoparticle solution was brought

to pH 9.5.[50] The oligonucleotide-modified gold nanoparticles were synthesized by derivatizing 6.4 ml of the alkaline gold nanoparticle solution with 3.5 ml of the 5′-(sulfanylalkanyl)-modified oligonucleotide solution. The solution was allowed to stand for 20 h at 40 °C followed by the addition of 4.8 ml of a 0.1 M NaCl, 10 mM phosphate buffer solution (pH 7). The solution was kept for further 2 days at 40 °C. The sample was centrifuged using screw cap micro tubes for 30 min at 14 000 rpm. The clear supernatant was removed and the red oily precipitate was washed two times with 8.4 ml of 0.1 M NaCl, 10 mM phosphate buffer solution (pH 7) and redispersed in 9.6 ml of a 0.1 M NaCl, 10 mM phosphate buffer solution (pH 8.5).

4-Amino-1-(2-deoxy-β-D-*erythro*-pentofuranosyl)-5-(prop-1-ynyl)pyrimidin-2*H*-2-one (2)

2′-Deoxy-5-iodocytidine (6.0 g, 17 mmol) (**4**) was dissolved in dry DMF (80 ml) under argon. Copper(I) iodide (99.99%, 652 mg, 3.3 mmol), tetrakis(triphenylphosphine)palladium(0) (1.7 g, 1.5 mmol) and triethylamine (4.8 ml, 3.4 g, 34.5 mmol) were added. The mixture was cooled in an ice-bath and propyne gas (99%) was introduced over 20 min under cooling. The reaction mixture was stirred overnight at r.t. TLC (silica gel, CH_3CN–H_2O, 95 : 5, containing 25% aq. NH_3 (2 ml) in 100 ml of solvent) showed a homogenous zone (2 developments) moving slightly faster than the starting material. The solvent was evaporated (70 °C) and co-evaporated with toluene (3 × 50 ml). The solid residue was suspended in CH_2Cl_2 and precipitated. The solid material was filtered and washed carefully with CH_2Cl_2, furnishing compound **2** (3.9 g, 86%) as a crude product. It was used in the next step without further purification. TLC (silica gel, CH_2Cl_2–MeOH, 9 : 1; 2 developments): R_f 0.30; λ_{max}(MeOH)/nm 297 (ε/dm^3 mol^{-1} cm^{-1} 4800), 227 sh (14 700) and 215 (16 900); δ_H (250.13 MHz; [d_6]DMSO; Me_4Si) 2.0 (5 H, m, CH_3 and 2 × 2′-H), 3.57 (1 H, m, 5′-H), 3.78 (1 H, m, 4′-H), 4.19 (1 H, m, 3′-H), 5.07 (1 H, m, 5′-OH), 5.20 (1 H, m, 3′-OH), 6.11 (1 H, 't', *J* 6.0, 1′-H), 6.94 and 7.72 (2 H, 2 br s, 2 × NH), 8.08 (1 H, s, 6-H).

4-Amino-1-[2-deoxy-5-*O*-(4,4′-dimethoxytrityl)-β-D-*erythro*-pentofuranosyl)]-5-(prop-1-ynyl)pyrimidin-2*H*-2-one (5)

Compound **2** (5.0 g, 18.8 mmol) was dissolved in dry pyridine (20 ml) and treated with 4,4′-dimethoxytriphenylmethyl chloride (6.0 g, 17.7 mmol). The reaction mixture was stirred overnight, diluted with CH_2Cl_2 (30 ml) and the reaction was quenched with 5% $NaHCO_3$ solution (40 ml). The aqueous layer was extracted with CH_2Cl_2 (3 × 40 ml) and the combined organic layers were dried (Na_2SO_4), filtered and the solvent evaporated. The oily residue was co-evaporated with toluene (3 × 50 ml) and purified by FC (silica gel, column 15 × 4 cm, CH_2Cl_2 → CH_2Cl_2–MeOH, 98 : 2 → 95 : 5 → 9 : 1) furnished a colourless solid (**5**; 8.5 g, 80%). (Found: C, 69.90; H, 5.81; N, 7.36%. $C_{33}H_{33}N_3O_6$ requires C, 69.83; H, 5.86; N, 7.40%); TLC (silica gel, CH_2Cl_2–MeOH, 9 : 1): R_f 0.5; λ_{max}(MeOH)/nm 296 (ε/dm^3 mol^{-1} cm^{-1} 11 000), 284 (11 200), 236 (38 300) and 214 (40 600); δ_H (250.13 MHz; [d_6]DMSO; Me_4Si) 1.84 (3 H, m, CH_3), 2.11 (2 H, m, 2 × 2′-H), 3.11 and 3.23 (2 H, 2 m, 2 × 5′-H), 3.74 (3 H, s, OCH_3), 3.93 (1 H, m, 4′-H), 4.26 (1 H, m, 3′-H), 5.32 (1 H, m, 3′-OH), 6.14 (1 H, 't', *J* 5.9, 1′-H), 6.90 (5 H, m, arom. H and NH of NH_2), 7.32 (9 H, m, arom. H), 7.72 (1 H, br s, NH of NH_2), 7.88 (1 H, br s, 6-H).

4-Benzoylamino-1-[2-deoxy-5-*O*-(4,4′-dimethoxytrityl)-β-D-*erythro*-pentofuranosyl)]-5-(prop-1-ynyl)pyrimidin-2*H*-2-one (6a)

Compound **5** (1.7 g, 3.0 mmol) was dissolved in anhyd. pyridine (20 ml). Then, *N*-ethyldiisopropylamine (1.8 ml, 10.4 mmol) and benzoic anhydride (1.15 g, 5.1 mmol) were added and the solution was stirred overnight at r.t. The solvent was evaporated and the oily residue was co-evaporated with toluene (3 × 20 ml). The resulting foam was purified by FC (silica gel, column 15 × 4 cm, CH_2Cl_2 → CH_2Cl_2–acetone, 9 : 1 → 4 : 1 → 1 : 1), furnishing a colourless solid (**6a**; 1.4 g, 68%). (Found: C, 71.43; H, 5.67; N, 6.07%. $C_{40}H_{37}N_3O_7$ requires C, 71.52; H, 5.55; N, 6.26%); TLC (silica gel, CH_2Cl_2: acetone, 1 : 1): R_f 0.7; λ_{max}(MeOH)/nm 298 (ε/dm^3 mol^{-1} cm^{-1} 7400), 282 (8300), 232 (41 600) and 211 (47 400); δ_H (250.13 MHz; [d_6]DMSO; Me_4Si) 1.69 (3 H, s, CH_3), 2.29 (2 H, m, 2′-H), 3.24 (2 H, m, 2 × 5′-H), 3.74 (3 H, s, OCH_3), 4.00 (1 H, m, 4′-H), 4.29 (1 H, m, 3′-H), 5.38 (1 H, m, 3′-OH), 6.12 (1 H, m, 1′-H), 6.90, 7.32, 8.01 (19 H, 3 m, arom. H and 6-H), 12.56 (1 H, br s, NH).

4-Benzoylamino-1-[2-deoxy-5-*O*-(4,4′-dimethoxytrityl)-β-D-*erythro*-pentofuranosyl)]-5-(prop-1-ynyl)pyrimidin-2*H*-2-one 3′-(2-cyanoethyl)diisopropylphosphoramidite (3a)

Compound **6a** (750 mg, 1.1 mmol) was dissolved in dry CH_2Cl_2 (10 ml). The mixture was treated with *N*-ethyldiisopropylamine (0.4 ml, 2.3 mmol) and (2-cyanoethyl)diisopropylphosphoramidochloridite (0.4 ml, 1.8 mmol) for 20 min at r.t. The solution was diluted with CH_2Cl_2 (10 ml) and poured into 5% aq. $NaHCO_3$ (50 ml). The aqueous layer was extracted with CH_2Cl_2 (3 × 50 ml), and the combined organic layers were dried (Na_2SO_4), filtered and evaporated. The residual foam was purified by FC (silica gel, column 10 × 5 cm, CH_2Cl_2–acetone, 9 : 1). Evaporation of the main zone afforded a yellowish foam (**3a**; 600 mg, 62%). (Found: C, 67.65; H, 6.29; N, 7.80%. $C_{49}H_{54}N_5O_8P$ requires C, 67.49; H, 6.24; N, 8.03%); TLC (silica gel, CH_2Cl_2–acetone, 9 : 1): R_f 0.7. δ_P ($CDCl_3$) 149.8, 150.3.

4-Acetylamino-1-[2-deoxy-5-*O*-(4,4′-dimethoxytrityl)-β-D-*erythro*-pentofuranosyl)]-5-(prop-1-ynyl)pyrimidin-2*H*-2-one (6b)

Compound **5** (5.0 g, 8.8 mmol) was dissolved in dry *N*,*N*-dimethylformamide (50 ml). Then, acetic anhydride (1.0 ml, 10.6 mmol) was added and the solution was stirred overnight at r.t. The solvent was evaporated and the oily residue was co-evaporated with toluene (3 × 20 ml). The resulting foam was purified by FC (silica gel, column 15 × 4 cm, CH_2Cl_2 → CH_2Cl_2–acetone, 9 : 1 → 4 : 1 → 1 : 1) furnishing a colourless foam (**6b**; 4.3 g, 80%). (Found: C, 69.00; H, 5.70; N, 6.76%. $C_{35}H_{35}N_3O_7$ requires C, 68.95; H, 5.79; N, 6.89%); TLC (silica gel, CH_2Cl_2–acetone, 1 : 1): R_f 0.5; λ_{max}(MeOH)/nm 309 (ε/dm^3 mol^{-1} cm^{-1} 6300), 282 (61 100), 236 (41 300) and 212 (38 500); δ_H (250.13 MHz; [d_6]DMSO; Me_4Si) 1.84 (3 H, s, CH_3), 2.20 (2 H, m, 2′-H), 2.35 (3 H, s, CH_3), 3.24 (2 H, m, 2 × 5′-H), 3.74 (3 H, s, OCH_3), 4.02 (1 H, m, 4′-H), 4.28 (1 H, m, 3′-H), 5.37 (1 H, d, *J* 4.25, 3′-OH), 6.06 (1 H, 't', *J* 6.2, 1′-H), 6.90 and 7.32 (13 H, 2 m, arom. H), 8.20 (1 H, s, 6-H), 9.2 (1 H, br s, NH).

4-Acetylamino-1-[2-deoxy-5-*O*-(4,4′-dimethoxytrityl)-β-D-*erythro*-pentofuranosyl)]-5-(prop-1-ynyl)pyrimidin-2*H*-2-one 3′-(2-cyanoethyl)diisopropylphosphoramidite (3b)

Compound **6b** (4.1 g, 6.7 mmol) was dissolved in anhyd. CH_2Cl_2 (10 ml). The mixture was treated with *N*-ethyldiisopropylamine (3.1 ml, 17.8 mmol) and (2-cyanoethyl)diisopropylphosphoramidochloridite (3.1 ml, 14.0 mmol) for 20 min at r.t. The solution was diluted with CH_2Cl_2 (10 ml) and poured into 5% aq. $NaHCO_3$ (50 ml). The aqueous layer was extracted with CH_2Cl_2 (3 × 50 ml), and the combined organic layers were dried (Na_2SO_4), filtered and evaporated. The residual foam was purified by FC (silica gel, column 10 × 5 cm, CH_2Cl_2–acetone, 4 : 1). Evaporation of the main zone afforded a white foam (**3b**; 3.7 g, 68%). (Found: C, 65.18; H, 6.39; N, 8.70%. $C_{44}H_{52}N_5O_8P$ requires C, 65.25; H, 6.47; N, 8.65%); TLC (silica gel, CH_2Cl_2–acetone, 4 : 1): R_f 0.7. δ_P ($CDCl_3$) 149.8, 150.4.

4-[(Dibutylaminomethylidene)amino]-1-[2-deoxy-5-*O*-(4,4′-dimethoxytrityl)-β-D-*erythro*-pentofuranosyl)]-5-(prop-1-ynyl)pyrimidin-2*H*-2-one (6c)

Compound **5** (250 mg, 0.44 mmol) was dissolved in MeOH (5 ml). Then, *N*,*N*-dibutylformamide dimethylacetal (500 µl) was added and the reaction mixture was stirred for 3 h at r.t. The solvent was evaporated and the oily residue was co-evaporated with toluene (3 × 20 ml) and acetone (1 × 10 ml). The resulting oil was purified by FC (silica gel, column 12 × 4 cm, CH_2Cl_2–acetone, 9 : 1 → 4 : 1 → 1 : 1) furnishing a colourless foam (**6c**; 195 mg, 62.7%). (Found: C, 71.38; H, 7.28; N, 7.78%. $C_{42}H_{50}N_4O_6$ requires C, 71.36; H, 7.13; N, 7.93%); TLC (silica gel, CH_2Cl_2–acetone, 1 : 1): R_f 0.5; λ_{max}(MeOH)/nm 340 (ε/dm^3 mol^{-1} cm^{-1} 21 200), 257sh (17 800), 236 (38 400); δ_H (250.13 MHz; [d_6]DMSO; Me_4Si) 0.92 (6 H, m, 2 × CH_3), 1.27 (4 H, m, 2 × CH_2), 1.57 (4 H, m, 2 × CH_2), 1.79 (3 H, s, CH_3), 2.12 (1 H, m, 2′-H), 2.29 (1 H, m, 2′-H), 3.15 (2 H, m, NCH_2), 3.46 (4 H, m, NCH_2 and 5′-H), 3.74 (6 H, s, 2 × OCH_3), 3.96 (1 H, m, 4′-H), 4.27 (1 H, m, 3′-H), 5.33 (1 H, d, *J* 4.09, 3′-OH), 6.14 (1 H, 't', *J* 5.8, 1′-H), 6.89 (4 H, m, arom. H), 7.32 (9 H, arom. H), 7.99 (1 H, s, 6-H), 8.58 (1 H, s, N=CH).

4-[(Dibutylaminomethylidene)amino]-1-[2-deoxy-5-*O*-(4,4′-dimethoxytrityl)-β-D-*erythro*-pentofuranosyl)]-5-(prop-1-ynyl)pyrimidin-2*H*-2-one 3′-[(2-cyanoethyl)-*N*,*N*-(diisopropyl)]phosphoramidite (3c)

Compound **6c** (100 mg, 0.14 mmol) was dissolved in anhyd. CH_2Cl_2 (10 ml). The mixture was treated with *N*,*N*-diisopropylethylamine (48 µl, 0.21 mmol) and (2-cyanoethyl)diisopropylphosphoramidochloridite (48 µl, 0.23 mmol) for 20 min at r.t. The solution was diluted with CH_2Cl_2 (10 ml) and poured into 5% $NaHCO_3$ solution (50 ml). The aqueous layer was extracted with CH_2Cl_2 (3 × 50 ml), and the combined organic layers were dried (Na_2SO_4), filtered and evaporated. The residual foam was purified by FC (silica gel, column 10 × 5 cm, CH_2Cl_2–acetone, 85 : 15). Evaporation of the main zone afforded a colourless foam (**3c**; 81 mg, 63%). TLC (silica gel, CH_2Cl_2–acetone, 9 : 1): R_f 0.7. δ_P ($CDCl_3$) 150.1, 149.5.

Acknowledgements

We thank Mrs E. Michalek, Dr K. I. Shaikh and Dr T. Koch from Roche Diagnostics GmbH for the measurement of the MALDI spectra, and Mrs K. Xu and Mr V. R. Sirivolu for reading the manuscript. Financial support from the Deutsche Forschungsgemeinschaft, Graduate School 612 and ChemBiotech, Münster, is gratefully acknowledged.

References

1 M. Mills, L. Lacroix, P. B. Arimondo, J.-L. Leroy, J. C. François, H. Klump and J.-L. Mergny, *Curr. Med. Chem.: Anti-Cancer Agents*, 2002, **2**, 627–644.
2 S. Nonin-Lecomte and J.-L. Leroy, *J. Mol. Biol.*, 2001, **309**, 491–506.
3 G. Manzini, N. Yathindra and L. E. Xodo, *Nucleic Acids Res.*, 1994, **22**, 4634–4640.
4 J.-L. Leroy, M. Guéron, J.-L. Mergny and C. Hélène, *Nucleic Acids Res.*, 1994, **22**, 1600–1606.
5 P. Catasti, X. Chen, L. L. Deaven, R. K. Moyzis, E. M. Bradbury and G. Gupta, *J. Mol. Biol.*, 1997, **272**, 369–382.
6 M. Guéron and J.-L. Leroy, *Curr. Opin. Struct. Biol.*, 2000, **10**, 326–331.
7 A. T. Phan, M. Guéron and J.-L. Leroy, *J. Mol. Biol.*, 2000, **299**, 123–144.
8 A. T. Phan and J.-L. Mergny, *Nucleic Acids Res.*, 2002, **30**, 4618–4625.
9 R. D. Wells, D. A. Collier, J. C. Hanvey, M. Shimizu and F. Wohlrab, *FASEB J.*, 1988, **2**, 2939–2949.
10 R. Langridge and A. Rich, *Nature*, 1963, **198**, 725–728.
11 K. Gehring, J.-L. Leroy and M. Guéron, *Nature*, 1993, **363**, 561–565.
12 C. H. Kang, I. Berger, C. Lockshin, R. Ratliff, R. Moyzis and A. Rich, *Proc. Natl. Acad. Sci. U. S. A.*, 1994, **91**, 11636–11640.
13 C. H. Kang, I. Berger, C. Lockshin, R. Ratliff, R. Moyzis and A. Rich, *Proc. Natl. Acad. Sci. U. S. A.*, 1995, **92**, 3874–3878.
14 L. Chen, L. Cai, X. Zhang and A. Rich, *Biochemistry*, 1994, **33**, 13540–13546.
15 J.-L. Mergny, L. Lacroix, X. Han, J.-L. Leroy and C. Hélène, *J. Am. Chem. Soc.*, 1995, **117**, 8887–8898.
16 X. Han, J.-L. Leroy and M. Guéron, *J. Mol. Biol.*, 1998, **278**, 949–965.
17 D. M. J. Lilley, *Biopolymers*, 1998, **48**, 101–112.
18 M. Edmonds, *Bioessays*, 1984, **6**, 212–216.
19 S. Robidoux, R. Klinck, K. Gehring and M. J. Damha, *J. Biomol. Struct. Dyn.*, 1997, **15**, 517–527.
20 S. Robidoux and M. J. Damha, *J. Biomol. Struct. Dyn.*, 1997, **15**, 529–535.
21 H. Kanehara, M. Mizuguchi, K. Tajima, K. Kanaori and K. Makino, *Biochemistry*, 1997, **36**, 1790–1797.
22 J.-L. Mergny and L. Lacroix, *Nucleic Acids Res.*, 1998, **26**, 4797–4803.
23 J. A. Brazier, J. Fisher and R. Cosstick, *Angew. Chem.*, 2006, **118**, 120–123.
24 L. Lacroix and J.-L. Mergny, *Arch. Biochem. Biophys.*, 2000, **381**, 153–163.
25 F. Seela and Y. He, 'Modified Nucleosides, Synthesis and Applications' in: *Organic and Bioorganic Chemistry*, ed. D. Loakes, Transworld Research Network, Kerala, India, 2002, pp. 57–85.
26 (*a*) B. C. Froehler, S. Wadwani, T. J. Terhorst and S. R. Gerrard, *Tetrahedron Lett.*, 1992, **33**, 5307–5310; (*b*) R. Eritja, E. Ferrer, R. Güimil and M. Orozco, *Nucleosides Nucleotides*, 1999, **18**, 1619–1621; (*c*) V. N. Soyfer and V. N. Potaman, *Triple-Helical Nucleic Acids*, Springer-Verlag, New York, 1995, pp. 161–162.
27 J. Sági, A. Szemzö, K. Ébinger, A. Szaboles, G. Sági, É Ruff and L. Ötvös, *Tetrahedron Lett.*, 1993, **34**, 2191–2194.
28 T. W. Barnes, III and D. H. Turner, *Biochemistry*, 2001, **40**, 12738–12745.
29 J. He and F. Seela, *Nucleic Acids Res.*, 2002, **30**, 5485–5496.
30 F. W. Hobbs, Jr., *J. Org. Chem.*, 1989, **54**, 3420–3422.
31 (*a*) V. Bhat, B. G. Ugarkar, V. A. Sayeed, K. Grimm, N. Kosora, P. A. Domenico and E. Stocker, *Nucleosides Nucleotides*, 1989, **8**, 179–183; (*b*) M. P. Reddy, N. B. Hanna and F. Farooqui, *Tetrahedron Lett.*, 1994, **35**, 4311–4314.
32 P. Strazewski, *Nucleic Acids Res.*, 1988, **16**, 5191.
33 F. Seela, S. Budow, H. Eickmeier and H. Reuter, *Acta Crystallogr., Sect. C: Cryst. Struct. Commun.*, 2007, **63**, o54–o57.

34 DNA synthesizer users' manual, Applied Biosystems, Weiterstadt, Germany, p. 392.
35 (*a*) J. J. Storhoff, R. Elghanian, R. C. Mucic, C. A. Mirkin and R. L. Letsinger, *J. Am. Chem. Soc.*, 1998, **120**, 1959–1964; (*b*) R. Jin, G. Wu, Z. Li, C. A. Mirkin and G. C. Schatz, *J. Am. Chem. Soc.*, 2003, **125**, 1643–1654.
36 C. A. Sprecher and W. C. Johnson, Jr., *Biopolymers*, 1977, **16**, 2243–2264.
37 N. Esmaili and J.-L. Leroy, *Nucleic Acids Res.*, 2005, **33**, 213–224.
38 S. Ahmed and E. Henderson, *Nucleic Acids Res.*, 1992, **20**, 507–511.
39 F. Seela and R. Kröschel, *Bioconjugate Chem.*, 2001, **12**, 1043–1050.
40 F. Seela, C. Wei and A. Melenewski, *Nucleic Acids Res.*, 1996, **24**, 4940–4945.
41 D. Collin and K. Gehring, *J. Am. Chem. Soc.*, 1998, **120**, 4069–4072.
42 M. Kaushik, N. Suehl and L. A. Marky, *Biophys. Chem.*, 2007, **126**, 154–164.
43 J.-L. Leroy, K. Gehring, A. Kettani and M. Guéron, *Biochemistry*, 1993, **32**, 6019–6031.
44 M. S. Shchepinov, K. U. Mir, J. K. Elder, M. D. Frank-Kamenetskii and E. M. Southern, *Nucleic Acids Res.*, 1999, **27**, 3035–3041.
45 R. H. E. Hudson, A. H. Uddin and M. J. Damha, *J. Am. Chem. Soc.*, 1995, **117**, 12470–12477.
46 N. Balgobin, A. Földesi, G. Remaud and J. Chattopadhyaya, *Tetrahedron*, 1988, **44**, 6929–6939.
47 P. Agback, C. Glemarec, C. Sund and J. Chattopadhyaya, *Tetrahedron*, 1992, **48**, 6537–6554.
48 H. Rosemeyer, E. Feiling, W. Nierling and F. Seela, *Nucleosides Nucleotides*, 1999, **18**, 1563–1564.
49 J. Turkevitch, P. C. Stevenson and J. Hillier, *Discuss. Faraday Soc.*, 1951, **11**, 55–75.
50 F. Seela and S. Budow, *Helv. Chim. Acta*, 2006, **89**, 1978–1985.
51 A. P. Alivisatos, K. P. Johnsson, X. Peng, T. E. Wilson, C. J. Loweth, M. P. Bruchez, Jr. and P. G. Schultz, *Nature*, 1996, **382**, 609–611.
52 N. L. Rosi, D. A. Giljohann, C. S. Thaxton, A. K. R. Lytton-Jean, M. S. Han and C. A. Mirkin, *Science*, 2006, **312**, 1027–1030.
53 M. S. Han, A. K. R. Lytton-Jean and C. A. Mirkin, *J. Am. Chem. Soc.*, 2006, **128**, 4954–4955.
54 (*a*) C. A. Mirkin, R. L. Letsinger, R. C. Mucic and J. J. Storhoff, *Nature*, 1996, **382**, 607–609; (*b*) R. Elghanian, J. J. Storhoff, R. C. Mucic, R. L. Letsinger and C. A. Mirkin, *Science*, 1997, **277**, 1078–1081.
55 M. S. Han, A. K. R. Lytton-Jean, B.-K. Oh, J. Heo and C. A. Mirkin, *Angew. Chem., Int. Ed.*, 2006, **45**, 1807–1810.
56 (*a*) F. Seela, A. M. Jawalekar, L. Chi and D. Zhong, *Chem. Biodiversity*, 2005, **2**, 84–91; (*b*) F. Seela, A. M. Jawalekar, L. Chi, D. Zhong and H. Fuchs, *Nucleosides, Nucleotides Nucleic Acids*, 2005, **24**, 843–846.
57 B. Beermann, E. Carillo-Nava, A. Scheffer, W. Buscher, A. M. Jawalekar, F. Seela and H.-J. Hinz, *Biophys. Chem.*, 2007, **126**, 124–131.
58 F. Seela and V. R. Sirivolu, *Helv. Chim. Acta*, 2007, **90**, 535–552.
59 (*a*) C. W. Tornøe, C. Christensen and M. Meldal, *J. Org. Chem.*, 2002, **67**, 3057–3064; (*b*) V. V. Rostovtsev, L. G. Green, V. V. Fokin and K. B. Sharpless, *Angew. Chem., Int. Ed.*, 2002, **41**, 2596–2599.
60 T. S. Seo, Z. Li, H. Ruparel and J. Ju, *J. Org. Chem.*, 2003, **68**, 609–612.
61 F. Seela and G. Becher, *Nucleic Acids Res.*, 2001, **29**, 2069–2078.

